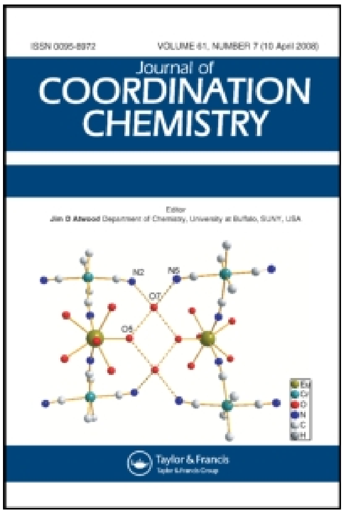

Journal of Coordination Chemistry
Publication details, including instructions for authors and subscription information:
http://www.informaworld.com/smpp/title~content=t713455674

Reactivity of the new potentially Binucleating Ligand, 2-(Acetichydrazido-*N*-Methylidene-α-Naphthol)-Benzothiazol, towards Manganese(II), Nickel(II), Cobalt(II), Copper(II) and Zinc(II) salts

Abdou Saad El-Tabl[a]; Saeyda Abdou El-Enein[a]
[a] Department of Chemistry, Faculty of Science, Menoufia University, Shebin El-Kom, Egypt

To cite this Article El-Tabl, Abdou Saad and El-Enein, Saeyda Abdou(2004) 'Reactivity of the new potentially Binucleating Ligand, 2-(Acetichydrazido-*N*-Methylidene-α-Naphthol)-Benzothiazol, towards Manganese(II), Nickel(II), Cobalt(II), Copper(II) and Zinc(II) salts', Journal of Coordination Chemistry, 57: 4, 281 — 294

To link to this Article: DOI: 10.1080/00958970410001664938

URL: http://dx.doi.org/10.1080/00958970410001664938

J. Coord. Chem., Vol. 57, No. 4, 10 March 2004, pp. 281–294

Taylor & Francis
Taylor & Francis Group

REACTIVITY OF THE NEW POTENTIALLY BINUCLEATING LIGAND, 2-(ACETICHYDRAZIDO-*N*-METHYLIDENE-α-NAPHTHOL)-BENZOTHIAZOL, TOWARDS MANGANESE(II), NICKEL(II), COBALT(II), COPPER(II) AND ZINC(II) SALTS

ABDOU SAAD EL-TABL* and SAEYDA ABDOU EL-ENEIN

Department of Chemistry, Faculty of Science, Menoufia University, Shebin El-Kom, Egypt

(Received 23 January 2003; Revised 16 May 2003; In final form 15 January 2004)

A new series of manganese(II), nickel(II), cobalt(II), copper(II) and zinc(II) complexes of 2-(acetichydrazido-*N*-methylidene-α-naphthol)-benzothiazol (H_2L) was prepared and characterized by elemental analysis, IR, UV–VIS, magnetic susceptibility, thermogravimetric analysis (TGA), molar conductance and ESR measurements. Molar conductances of the complexes in DMF are commensurate with their nonelectrolytic nature. IR spectral data show that the ligand can be bidentate and/or tridentate. ESR spectra of the solid copper(II) Complexes **8** and **9** show a $d_{x^2-y^2}$ ground state with covalent character. The fungicidal activities of the ligand and its metal complexes against *Aspergillus niger* and *Fusarium oxysporum* are discussed.

Keywords: Complexes; Synthesis; Conductivity; Magnetic properties; Thermal analysis; Spectroscopic studies

Hydrazones and their transition metal complexes are investigated because of their analytical, industrial and pharmacological importance. One example is the tridentate ligand, salicylaldehyde benzoylhydrazone (H_2Sb), which has mild bacteriostatic activity [1]; analogues have been investigated as potential oral iron-chelating drugs for genetic disorders such as thalassaemia [2]. The copper(II) complex $[Cu(HSb)Cl] \cdot H_2O$ was shown to be a potent inhibitor for DNA synthesis and cell growth, more potent than the unbound moiety [3,4]. Interest is focused solely on the preparation and characterization of related ligands and their metal(II) complexes. This article reports a new series of Mn(II), Ni(II), Co(II), Cu(II) and Zn(II) complexes of 2-(acetichydrazido-*N*-methylidene-α-naphthol)-benzothiazol that have been prepared and characterized spectroscopically.

---

*Corresponding author. E-mail: asaeltabl@yahoo.com

ISSN 0095-8972 print: ISSN 1029-0389 online
DOI: 10.1080/00958970410001664938

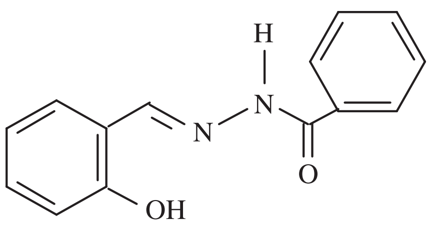

(H_2Sb)

EXPERIMENTAL

Reagent-grade chemicals were used without further purification. C, H and N were determined at the Analytical Unit of Cairo University, Egypt. Standard methods [5] were used for determining the metal ions. IR spectra of the ligand and its metal(II) complexes were recorded on a Perkin-Elmer 681 spectrophotometer using KBr and CsBr discs. Electronic spectra (200–900 nm) were measured (nujol mull and DMF solution) with a Perkin-Elmer 550 spectrophotometer. The magnetic susceptibilities were measured at 25°C with a Johnson Matthey balance. Diamagnetic corrections were made using Pascal's constant [6]. Magnetic susceptibilities were determined by using $\mu_{\text{eff}} = 2.84 \cdot \sqrt{\chi_{\text{M}}\text{corr}.T}$. The molar conductance measurements were carried out in DMF solution (10^{-3} M) using a Bibby conductimeter MCl. Thermogravimetric analysis (TGA) was carried out in air using a Shimadzu DT-30 thermal analyzer from 27 to 700°C. The ESR spectra of the solid complexes were obtained at room temperature using a Varian E-109 spectrophotometer, with DPPH as the standard. TLC of all of the compounds was used to confirm their purity.

Preparation of the Ligand and its Metal(II) Complexes

Benzothiazol-2-ylacetohydrazide was prepared as described previously [7].

Preparation of H_2L (1)

2-(Acetichydrazido-*N*-methylidene-α-naphthol)-benzothiazol (**1**) was prepared by refluxing equimolar amounts of benzothiazol-2-ylacetohydrazide (5.0 g, 0.03 mol) and naphthaldehyde (4.9 g, 0.03 mol) in ethanol (100 cm^3) for 2 h with stirring. The yellow product obtained was filtered off, washed several times with ethanol and then recrystallized from dioxane and dried in air. Analytical data are given in Table I.

Preparation of Complexes 2, 4, 6, 8 and 10

To the ligand (5.0 g, 0.01 mol) in ethanol (30 cm^3) was added 3.49 g (0.01 mol) of $Ni(OAc)_2 \cdot 4H_2O$ (complex **2**), 3.4 g (0.01 mol) of $Co(OAc)_2 \cdot 4H_2O$ (complex **4**), 3.41 g (0.01 mol) of $Mn(OAc)_2 \cdot 4H_2O$ (complex **6**), 2.8 g (0.01 mol) of $Cu(OAc)_2 \cdot H_2O$ (complex **8**), or 3.0 g (0.01 mol) of $Zn(OAc)_2 \cdot 2H_2O$ and triethylamine (3–5 drops) (complex **10**), in the same solvent (50 cm^3). The mixture was refluxed with stirring

TABLE I Analytical and physical data for the ligand and its metal(II) complexes

Compound no.	*Formulation*	*Colour*	*Yield*	*mp*	*Found (Calcd.)*				Λ ($ohm^{-1} cm^2 mol^{-1}$)	μ_{eff} (BM)
			(%)	(°C)	*C*	*H*	*N*	*M*		
1	$[H_2L]$ $C_{20}H_{15}N_3SO_2$	Yellow	85	210	66.2 (66.4)	4.2 (4.1)	11.6 (11.5)	– –	7.2	–
2	$[(HL)Ni(OAc)(H_2O)_2]$ $C_{22}H_{21}N_3SO_6Ni$	Brown	80	> 300	51.6 (51.4)	4.1 (4.1)	7.9 (8.2)	11.6 (11.5)	7.5	2.93
3	$[(H_2L)_2Ni(OAc)_2]$ $C_{44}H_{36}N_6S_2O_8Ni$	Yellowish brown	82	235	59.0 (58.7)	3.8 (4.0)	9.0 (9.5)	6.7 (6.6)	23.9	3.0
4	$[(HL)Co(OAc)(H_2O)_2]$ $C_{22}H_{21}N_3SO_6Co$	Brown	85	> 300	51.6 (51.4)	4.0 (4.1)	8.1 (8.0)	11.5 (11.6)	4.1	4.91
5	$[(H_2L)_2Co(OAc)_2]$ $C_{44}H_{36}N_6S_2O_8Co$	Brown	83	> 300	58.7 (58.8)	4.0 (4.0)	9.2 (9.3)	6.4 (6.6)	6.1	4.95
6	$[(HL)Mn(OAc)(H_2O)_2]$ $C_{22}H_{21}N_3SO_6Mn$	Dark brown	75	> 300	52.0 (51.8)	4.1 (4.1)	8.3 (8.2)	11.0 (10.8)	5.5	6.3
7	$[(H_2L)_2Mn(OAc)_2]$ $C_{44}H_{36}N_6S_2O_8Mn$	Brown	78	> 300	59.0 (59.1)	4.0 (3.9)	9.1 (9.3)	6.0 (6.1)	12.1	6.1
8	$[(HL)Cu(OAc)(H_2O)_2]$ $C_{22}H_{21}N_3SO_6Cu$	Brown	85	278	50.9 (51.0)	4.2 (4.1)	8.0 (8.1)	11.2 (11.4)	36.5	1.70
9	$[(HL)_2Cu \cdot 2H_2O] \cdot H_2O$ $C_{40}H_{34}N_6S_2O_7Cu$	Dark brown	80	> 300	57.2 (57.4)	3.7 (3.8)	9.9 (10.0)	7.6 (7.7)	13.6	1.67
10	$[(HL)_2Zn \cdot 2H_2O] \cdot 2H_2O$ $C_{40}H_{36}N_6S_2O_8Zn$	Pale brown	82	> 300	55.9 (56.0)	4.1 (4.2)	9.6 (9.8)	7.5 (7.6)	4.4	Diamag.
11	$[(HL)_2Zn]$ $C_{40}H_{28}N_6S_2O_4Zn$	Orange	80	> 300	61.0 (61.1)	3.5 (3.6)	10.5 (10.6)	8.1 (8.3)	7.0	Diamag.

for 2 h. When the precipitate appeared, it was removed by filtration, washed with ethanol, and dried *in vacuo* over P_2O_5. Analytical data are given in Table I.

Preparation of Complexes 3, 5, 7, 9 and 11

These complexes were prepared by mixing 10 g (0.02 mol) of the ligand in ethanol (50 cm^3) with 3.4 g (0.01 mol) of $Ni(OAc)_2 \cdot 4H_2O$ (Complex **3**), 3.4 g (0.01 mol) of $Co(OAc)_2 \cdot 4H_2O$ (complex **5**), 3.41 g (0.01 mol) of $Mn(OAc)_2 \cdot 4H_2O$ (Complex **7**), 2.8 g (0.01 mol) of $Cu(OAc)_2 \cdot H_2O$ and triethylamine (3–5 drops) (Complex **9**) or 3.0 g (0.01 mol) of $Zn(OAc)_2 \cdot 2H_2O$ (Complex **11**), in the same solvent (50 cm^3), using the above procedure. The product was removed by filtration, washed with ethanol and dried *in vacuo* over P_2O_5. The analytical data are given in Table I.

RESULTS AND DISCUSSION

All the solid complexes are coloured, stable at room temperature, nonhygroscopic, insoluble in water and alcoholic solvents, partially soluble in common organic solvents such as $CHCl_3$ and appreciably soluble in DMF and DMSO. The analytical and physical data (Table I) and spectral data (Tables II and III) are compatible with the proposed structures (Fig. 1). The molar conductances of the complexes in 10^{-3} M DMF at 25°C are in the range 4.1–36.5 ohm^{-1} cm^2 mol^{-1}, indicating their nonelectrolytic nature [8,9].

IR Spectra

The IR spectral data of the ligand and its metal(II) complexes are listed in Table II. The spectrum of the ligand shows two medium bands at 3200 and 3100 cm^{-1}, assigned to ν(N–H). The relatively strong bands at 1675, 1620 and 1045 cm^{-1} are attributed to ν(C=O), ν(C=N) and ν(N–N), respectively [10]. The bands at 1575 and 1600 cm^{-1} are assigned to ν(C=N) of the thiazole ring and $\nu(C{=}C)_{Ar}$, respectively. The spectra of the complexes show bands due to ν(C=O) and ν(C=N) that are shifted by approximately 5–10 and 5–7 cm^{-1}, respectively, to lower frequency compared to the ligand, except for Complexes **7** and **11** (Table II). The ν(C=O) appears at lower frequency indicating that this group participated in the coordination. Two strong bands appear at 970–1010 and 1590–1598 cm^{-1}, assigned to ν(N–N) and ν(C=C), respectively [11]. The bands in the 3045–3200 cm^{-1} range are due to the ν(N–H) group. The spectra of the complexes also display new bands in the 600–670 and 510–565 cm^{-1} ranges, corresponding to ν(M–O) and ν(M–N), respectively [12]. The occurrence of the ν(OH) band at lower frequency (3085–3360 cm^{-1}) (Table II) in comparison with the range expected for the free hydroxyl groups (3500–3650 cm^{-1}) may indicate hydrogen bonding in the free ligand and its metal(II) Complexes **5**, **9** and **10** or M–O bonding as in Complex **7** [13,14]. The ν(OH) frequency in Complex **7** is the lowest, suggesting that the Mn–O bonding is stronger compared to the M–O bonding in the other complexes presented here, as expected from Pearson's concepts of 'hard and soft acids and bases' [15]. The involvement of the hydroxyl oxygen in the coordination is further supported by the shift of the ν(C–O) band to lower frequency upon coordination [16]. Complexes **2**, **4**, **6**, **8**, **9** and **10** show a broad band in the 3360–3650 cm^{-1} range; its absence in the

TABLE II IR spectral (cm^{-1}) assignment of the ligand and its metal(II) complexes

No.	$\nu(O{-}H)$	$\nu(N{-}H)$	$\nu(OAc)$	$\nu(C{=}N)$	$\nu(C{=}O)$	$\nu(C{=}N)ring$	$\nu(C{=}C)$	$\nu(C{-}O)$	$\nu(N{-}N)$	$\nu(M{-}N)$	$\nu(M{-}O)$
1	3360–3140	3200, 3100	–	1620	1675	1575	1600	1370	1045	–	–
2	3340–3120 3650–3360	3200, 3140	1568, 1410	1615	1665	1570	1595	1355	1005	565	625
3	3280–3100	3185, 3060	1572, 1385	1613	1669	1570	1592	1368	1010	535	620
4	3260–3150 3560–3390	3190, 3050	1580, 1405	1615	1668	1572	1590	1358	975	545	610
5	3350–3000	3190, 3050	1570, 1390	1618	1670	1570	1598	1365	960	550	600
6	3210–3085 3520–3370	3165, 3045	1565, 1395	1615	1665	1570	1592	1345	970	535	610
7	3250–3090	3200, 3045	1580, 1400	1617	1675	1572	1598	1355	970	560	600
8	3620–3350	3190, 3095	1565, 1410	1614	1665	1572	1595	1655	980	565	620
9	3300–3120 3600–3390	–	–	1615	–	1570	1590	1368	1000	510	650
10	3330–3150 3630–3375	–	–	1615	–	1565	1595	1365	975	540	630
11	–	3200, 3045	–	1613	1675	1560	1598	1355	970	560	670

TABLE III Electronic spectra of the ligand and its metal(II) complexes

Compound no.	*Medium*	λ_{max} (nm)
1	DMF	310 ($\log \varepsilon = 4.8$)
		230 ($\log \varepsilon = 6.5$)
2	Nujol mull	870, 642, 435, 330
	DMF	855 ($\log \varepsilon = 2.7$)
		625 ($\log \varepsilon = 2.0$)
		400 ($\log \varepsilon = 3.0$)
		292 ($\log \varepsilon = 3.9$
3	Nujol mull	880, 635, 425, 350
	DMF	873 ($\log \varepsilon = 4.2$)
		615 ($\log \varepsilon = 3.0$)
		390 ($\log \varepsilon = 2.0$)
		295 ($\log \varepsilon = 3.7$)
4	Nujol mull	880, 482, 410
	DMF	872 ($\log \varepsilon = 2.6$)
		479 ($\log \varepsilon = 4.9$)
		405 ($\log \varepsilon = 5.7$)
5	Nujol mull	878, 470, 415
	DMF	870 ($\log \varepsilon = 2.7$)
		465 ($\log \varepsilon = 5.0$)
		412 ($\log \varepsilon = 5.6$)
6	Nujol mull	660, 525, 430
	DMF	635 ($\log \varepsilon = 1.96$)
		498 ($\log \varepsilon = 2.5$)
		380 ($\log \varepsilon = 3.0$)
7	Nujol mull	650, 540, 435
	DMF	635 ($\log \varepsilon = 2.0$)
		530 ($\log \varepsilon = 2.4$)
		385 ($\log \varepsilon = 2.98$)
8	Nujol mull	635, 520, 415
	DMF	610 ($\log \varepsilon = 2.4$)
		510 ($\log \varepsilon = 2.6$)
		405 ($\log \varepsilon = 3.1$)
9	Nujol mull	630, 525, 410
	DMF	620 ($\log \varepsilon = 2.1$)
		515 ($\log \varepsilon = 2.2$)
		400 ($\log \varepsilon = 2.9$)

other complexes may be attributed to ν(OH) of the water molecules [17]. The complexes show bands in the 1345–1368 cm^{-1} range corresponding to the ν(C–O) vibration [18]. The $\nu_a(CO_2)$ and $\nu_s(CO_2)$ bands of the free acetate ions are at 1560 and 1416 cm^{-1}, respectively. In monodentate coordination ν(C=O) is found at higher energy than $\nu_a(CO_2)$ and ν(C–O) is lower than $\nu_s(CO_2)$. As a result, the separation between the two ν(CO) bands is much larger in monodentate complexes than in the free ion [19]. For Complexes **2**, **3**, **4**, **5**, **6**, **7** and **8** the $\nu_a(CO_2)$ appears between 1565 and 1580 cm^{-1} and $\nu_s(CO_2)$ between 1385 and 1410 cm^{-1}, indicating monodentate coordination to the metal ion [19].

Electronic Spectra

Electronic spectral data for the ligand and its metal(II) complexes are summarized in Table III. The spectrum of the ligand in DMF solution exhibits bands at 310 nm

($\log \varepsilon = 4.8$, where ε is in $\mathrm{L\,mol^{-1}cm^{-1}}$) and 230 nm ($\log \varepsilon = 6.5$) corresponding to $n \rightarrow \pi^*$ and $\pi \rightarrow \pi^*$ transitions within the ligand molecule [20]. Nickel(II) complex **2** exhibits bands in a nujol mull at 330, 435, 642 and 870 nm, and in DMF the bands appear at 292, 400, 625 and 855 nm; Complex **3** shows bands in the nujol mull located at 350, 425, 635 and 880 nm, and in DMF the peaks appear at 295, 390, 615 and 873 nm. The first peak is within the ligand and the other peaks correspond to $^3A_{2g} \rightarrow T_{1g}(p)$ (ν_3), $^3A_{2g} \rightarrow {}^3T_{1g}$ (ν_2) and $^3A_{2g} \rightarrow {}^3T_{2g}$ (ν_1) transitions of six-coordinate nickel(II) complexes [12]. The ν_2/ν_1 ratios for the complexes are 1.40 and 1.42, respectively, which are less than the usual range of 1.5–1.75 indicating distorted octahedral nickel(II) complexes [21,22]. The electronic spectrum of the cobalt(II) Complex **4** in nujol mull exhibits bands at 410, 482 and 880 nm, and in DMF it displays bands at 405, 479 and 872 nm; Complex **5** shows bands in nujol mull at 415, 470 and 878 nm, and in DMF the bands appear at 412, 465 and 870 nm. These bands are assigned to $^4T_{1g} \rightarrow {}^4T_{1g}(p)$ (ν_3), $^4T_{1g} \rightarrow {}^4A_{2g}$ (ν_2) and $^4T_{1g} \rightarrow {}^4T_{2g}$ (ν_1) transitions, respectively, indicating octahedral cobalt(II) complexes [23]. The lower value of ν_2/ν_1 (1.83 and 1.87, respectively) may be due to distortion of the octahedral structure [24], consistent with the very broad nature of the ν_1 band, which may be best assigned to the envelope of the transitions from ^4E_g ($^4T_{1g}$) to the components ($^4B_{2g}$ and ^4E_g) of $^4T_{2g}$, characteristic of a tetragonally distorted octahedral environment [24]. Manganese(II) Complex **6** in nujol mull exhibits bands at 660, 525 and 430 nm, and in DMF at 635, 498 and 380 nm; Complex **7** in nujol mull shows bands at 650, 540 and 435 nm, and in DMF at 635, 530 and 385 nm, assigned to $^5E_g \rightarrow {}^5E_{2g}$ and spin forbidden transitions for octahedral complexes [25]. The copper(II) Complex **8** in nujol mull gives bands at 635, 520 and 415 nm, and in DMF the bands appear at 610, 510 and 405 nm; Complex **9** in nujol mull gives bands at 630, 525 and 410 nm, and in DMF at 620, 515 and 400 nm assigned to $^2B_1 \rightarrow {}^2B_2$, $^2B_1 \rightarrow {}^2E$ and $O \rightarrow Cu$ charge transfer transition, respectively, indicating a distorted tetragonal structure [25–28]. A comparison of the electronic spectra of the complexes in solution and nujol mull indicates retention of geometry in solution.

Magnetic Moments

The magnetic moments for the metal(II) complexes are shown in Table I. Nickel(II) Complexes **2** and **3** show values of 2.93 and 3.0 BM, indicating octahedral geometry [29]. Cobalt(II) Complexes **4** and **5** have values of 4.91 and 4.95 BM, indicating high-spin octahedral cobalt(II) geometry [30]. Manganese(II) complexes **6** and **7** show values of 6.3 and 6.1 BM, characteristic of a high-spin octahedral geometry [31]. Copper(II) Complexes **8** and **9** show values of 1.70 and 1.67 BM, indicating distorted tetragonal structure [32,33]. These values are well below the normal value (1.73 BM) attributed to antiferromagnetic exchange interactions between neighbouring copper(II) ions [31,34]. Zinc(II) Complexes **10** and **11** are diamagnetic [33].

Electron Spin Resonance (ESR)

The ESR spectral data (Table IV) for the solid Complexes **8** and **9** at room temperature are characteristic of a monomer, d^9 configuration with a $d_{x^2-y^2}$ ground state, which is the most common for copper(II) complexes [27,35,36]. Complexes **8** and **9** show $g_{\parallel} > g_{\perp} > 2.04$, indicting a tetragonal distortion [37,38] corresponding to elongation

TABLE IV ESR parameters of the copper(II) complexes

Compound no.	$g_{\parallel}$	$g_{\perp}$	g_{iso}[a]	G[b]	ΔE_{xy}[c] (cm^{-1})	ΔE_{xz}[c] (cm^{-1})	$k_{\perp}^2$	$k_{\parallel}^2$	k
8	2.18	2.06	2.1	3.0	15.738	19.230	0.55	0.51	0.68
9	2.17	2.05	2.09	3.4	15.873	19.047	0.59	0.40	0.47

[a] $g_{iso} = 2g_{\perp} + g_{11}/3$.
[b] $G = (g_{\parallel} - 2)/(g_{\perp} - 2)$.
[c] Values × $10^3\,cm^{-1}$.

along the fourfold symmetry axis z. The g-values are related by the expression [32,39] $G = (g_{\parallel} - 2)/(g_{\perp} - 2)$. If $G > 4.0$, then the local tetragonal axes are aligned parallel or only slightly misaligned, if $G < 4.0$, the significant exchange coupling is present. The complexes show a G-value smaller than 4.0, indicating spin exchange interactions between the copper(II) ions.

The g-values of the copper(II) complexes with a $^2B_1$ ground state ($g_{\parallel} > g_{\perp}$) may be expressed by [38,39]:

$$g_{\parallel} = 2.002 - \frac{(8k_{\parallel}^2\lambda_o)}{(\Delta E_{xz})} \tag{1}$$

and

$$g_{\perp} = 2.002 - \frac{(2k_{\perp}^2\lambda_o)}{(\Delta E_{xy})} \tag{2}$$

$$k_{\parallel}^2 = \frac{(g_{\parallel} - 2.002)\Delta E_{xz}}{8\lambda_o} \tag{3}$$

$$k_{\perp}^2 = \frac{(g_{\perp} - 2.002)\Delta E_{xy}}{2\lambda_o} \tag{4}$$

$$k^2 = \frac{(k_{\parallel}^2 + 2k_{\perp}^2)}{3} \tag{5}$$

where $k_{\parallel}$ and $k_{\perp}$ are the parallel and perpendicular components, respectively, of the orbital reduction factor (k), λ_o is the spin–orbit coupling constant ($-828\,cm^{-1}$) for free copper, and ΔE_{xy} and ΔE_{xz} are the electron transition energies of $^2B_2 \leftarrow {}^2B_1$ and $^2E \leftarrow {}^2B_1$, respectively. For the purpose of calculation, we have assumed that the maximum in the band corresponds to ΔE_{xy} and that ΔE_{xz} can be taken from the wavelength of the band. From the above relations, the orbital reduction factors ($k_{\parallel}$, $k_{\perp}$ and k), which are a measure of covalency, can be calculated. For an ionic environment, $k = 1$ and for a covalent environment $k < 1$; the lower the value of k, the greater is the covalent character. The low values of k (Table IV) for the complexes are indicative of a covalent nature [40–47]. Complex **9** shows more covalency (O_4N_2 chromophore) than **8** (O_5N chromophore). Kivelson and Neiman [48] noted that for an ionic environment $g_{\parallel} \geq 2.3$ and for a covalent environment $g_{\parallel} < 2.3$. Theoretical work by Smith [49] seems to confirm this view. The $g_{\parallel}$ values reported here show a covalent bond character. The ESR spectrum of the solid cobalt(II) Complex **5** at room temperature shows a nonaxial type with a weak signal in the low-field region corresponding to $g_x = 2.17$ and two features in the high-field region due to $g_y = 2.05$ and $g_z = 2.04$. The g-values suggest an octahedral structure [31], $g_x > g_y > g_z$ and $(g_y - g_z)/(g_x - g_y)$ is lower than unity, indicating a $d_{x^2-y^2}$ ground state [50]. However, the spectrum of the solid manganese(II) Complex **7** shows six isotropic lines characteristic of an unpaired electron interacting with a nucleus of spin 5/2. The g-value is isotropic and equal to 2.0028, and the hyperfine coupling constant (A_{iso}) is equal to 87G [51,52].

Thermogravimetric Analysis (TGA)

Because the IR spectra indicate the presence of water molecules, thermal analysis was undertaken to ascertain their nature. The TGA curves for the complexes in the 20–700°C range show that all the complexes are thermally stable up to 50°C, when dehydration begins, and Complexes **2** and **4** are stable up to 125°C. The principal thermogravimetric data are collected in Table V. The thermal decomposition of the Complexes **2**, **4**, **6**, **9** and **10** take place in three main stages which can be explained as follows:

1. Dehydration of Complexes **9** and **10** takes place at 80 and 90°C, respectively [42,53–56], with weight loss corresponding to one H_2O for **9** and two H_2O for **10**.
2. The second step corresponds to loss of two moles of coordinated water for Complexes **2**, **4**, **6**, **8**, **9** and **10** and coordinated acetate for Complexes **2**, **4**, **6** and **8** [46–53,56], confirmed by the percentage weight loss (Table V). This experiment indicates two kinds of water (hydration and coordination) in Complexes **9** and **10**;

TABLE V TGA analysis for some metal(II) complexes

Compound no.	*Temp.* (°C)	*Wt. loss* (%)		*Assignment*
		Calcd.	*Found*	
2	125	7.0	6.8	Loss of coordinated water
	320	12.3	12.0	Loss of acetate group
	370–425	27.6	27.9	Break up of five-membered chelate ring
	620	24.6	24.8	Decomposition of the complex with the formation of NiO
4	137	7.1	6.7	Loss of coordinated water
	325	12.1	11.9	Loss of acetate group
	350–450	27.6	27.8	Break up of five-membered chelate ring
	560	24.5	24.7	Decomposition of the complex with the formation of CoO
6	150	7.0	7.1	Loss of coordinated water
	310	12.4	12.2	Loss of acetate group
	320–500	27.1	27.7	Break up of five-membered chelate ring
	610	23.7	23.2	Decomposition of the complex with the formation of MnO
9	80	2.1	1.9	Dehydration process
	150	4.4	5.0	Loss of coordinated water
	300–420	30.5	30.7	Break up of five-membered chelate ring
	530	14.5	14.2	Decomposition of the complex with the formation of CuO
10	90	4.2	4.1	Dehydration process
	220	4.4	4.1	Loss of coordinated water
	320–480	15.4	15.2	Break up of five-membered chelate ring
	600	11.1	11.2	Decomposition of the complex with the formation of ZnO

the hydration water helps the loss of coordinated water at lower temperatures 150 and 220°C.

3. TGA plots indicate that decomposition begins by fission of the coordinated bond Cu $\leftarrow$ N and chelate rings (six and five, respectively), confirmed by the percentage weight loss (Table V). The thermochemical changes of Complex **10** can thus be represented by the following equations.

$$[(HL)_2Zn \cdot 2H_2O] \cdot 2H_2O \xrightarrow{90^\circ C} [(HL)_2Zn \cdot 2H_2O] + 2H_2O$$

$$[(HL)_2Zn \cdot 2H_2O] \xrightarrow{220^\circ C} [(HL)_2Zn] + 2H_2O$$

$$[(HL)_2Zn] \xrightarrow{600^\circ C} ZnO + \text{organic residues}$$

As the temperature increases, the organic constituents of the complexes start to decompose, finally leaving the metal oxides (620–530°C).

Testing of Biological Activity

The fungicidal activities of the ligand and its metal complexes on *Aspergillus niger* and *Fusarium oxysporium* were evaluated using the agar plate technique [57]. The compounds tested were dissolved in DMSO to give a 10 000 ppm stock solution. From the stock solution the required concentration levels (100, 200, 500 ppm) were prepared by appropriate dilutions. The solutions at the appropriate concentrations were placed in Petri dishes and set aside for 1 h to ensure proper setting of the medium. Spores were taken from an 8-day-old culture of the fungi. The selected spores were planted at the centre of each Petri dish. The inoculated dishes were kept in an incubator at 27°C and the diameters of the resulting fungi colonies were measured with a millimetre scale after 3 and 5 days for *A. niger* and *F. oxysporium*, respectively. Table VI indicates that both the ligand and the metal complexes exhibited increasing fungitoxic activity with increasing concentration, and the complexes displayed higher toxicity against *A. niger* compared with the ligand. The complexes of Co(II) (**4**) and Cu(II) (**8**) display significantly higher fungitoxic activity against *F. oxysporum* than the ligand at all concentrations used. However, the Ni(II) Complex **2** shows higher toxicity against *A. niger*. The other complexes show a moderate toxic effect against the

TABLE VI Fungicidal activities of various concentrations of the ligand and its metal complexes on the growth (*G*) of *Aspergillus niger* and *Fusarium oxysporum* as indicated by the percentage of growth inhibition (*I*) (the data are the mean values of three replicates)

Compound	*Aspergillus niger*						*Fusarium oxysporum*					
	100 ppm		*200 ppm*		*500 ppm*		*100 ppm*		*200 ppm*		*500 ppm*	
	G (mm)	*I* (%)	*G* (mm)	*I* (%)	*G* (mm)	*I* (%)	*G* (mm)	*I* (%)	*G* (mm)	*I* (%)	*G* (mm)	*I* (%)
1	35.2	5.6	30.2	26.3	21.0	37.2	35.0	6.8	31.2	8.9	23.0	30.0
2	42.5	34.2	40.1	36.5	25.3	65.5	45.5	6.0	42.3	12.0	30.7	32.0
4	39.3	14.5	35.2	25.4	23.5	61.7	50.0	17.3	47.5	20.1	29.1	54.0
8	38.9	10.2	33.3	27.5	22.7	51.5	50.3	17.1	45.2	26.0	28.0	51.0
7	80.2	3.4	83.0	1.7	85.0	3.8	72.0	3.0	70.2	4.5	72.0	1.5
10	45.0	33.8	40.0	41.8	23.0	66.1	48.5	4.9	42.0	8.7	30.0	34

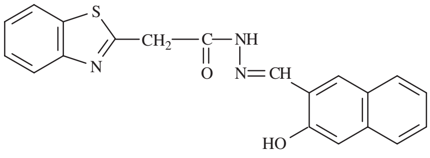

H_2L(1)

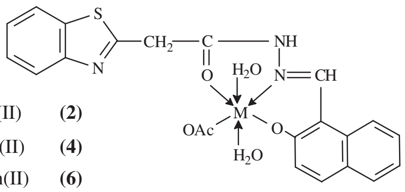

M = Ni(II) **(2)**
M = Co(II) **(4)**
M = Mn(II) **(6)**
M = Cu(II) **(8)**

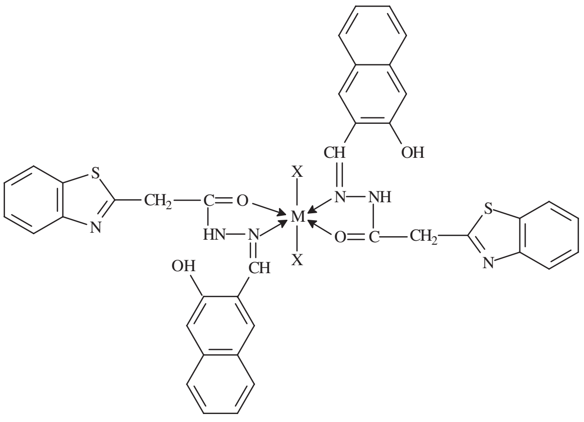

M = Ni(II) X = OAc **(3)**
M = Co(II) X = OAc **(5)**

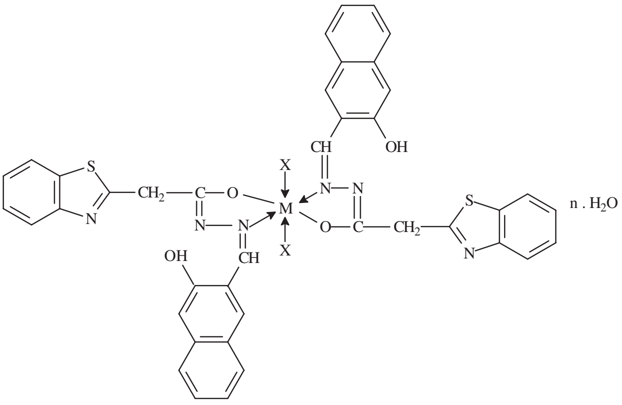

M = Cu(II) X = H_2O n = H_2O **(9)**
M = Zn(II) X = H_2O n = $2H_2O$ **(10)**

FIGURE 1 Structures of Ligand **1** and Complexes **2**–**11**.

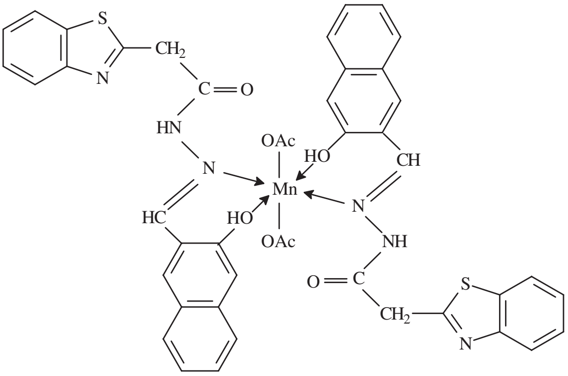

(7)

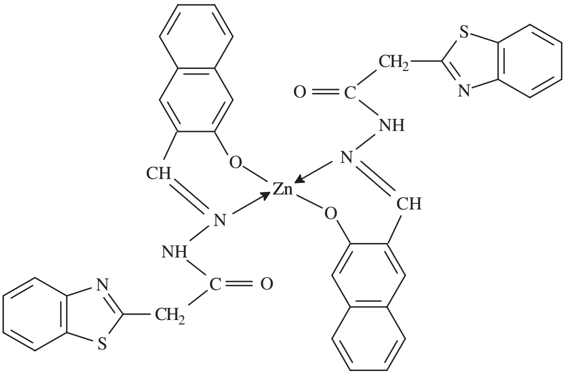

(11)

FIGURE 1 Continued.

fungal strain in comparison to the ligand alone. Aqueous ions of all the metals tested showed a significant lower growth inhibition in comparison with the complexes being studied (Table VI).

In conclusion, the metal complexes in most cases exhibit higher fungal toxicity in comparison to either the ligand or metal ions. Physico-chemical complexation between the aqueous metal ions (cations) and the anionic constituents of the fungal cell wall is predicted, which would lead to decreasing metal uptake and hence decreasing toxicity. However, metal complexation might facilitate entrance into the fungal cells and exert metal toxic action on the metabolic activity of the fungal cells resulting from the complex and inactivation of cellular functional macromolecules. The differential toxicity of the different metal ions was studied extensively and attributed to the chemical properties of the metal ions, their electronegativity, and the stability of the complex.

To date, no diffractable crystals have been grown, but we hope that in the future we will achieve crystals of complexes of the various types presented here. On the basis of elemental analyses, magnetic susceptibilities, molar conductances, IR and UV–VIS spectra, ESR measurements and TGA, the structures proposed are those shown in Fig. 1.

References

[1] H.A. Offe, W. Siefken and G. Domagk, *Naturforsch. Z., Teil B* **7**, 446 (1952).
[2] D. Richardson, E. Baker, P. Ponka, P. Wilairat, M.L. Vitoto and J. Webb, In: S. Fucharoen, P.T. Rowley and N.W. Poul (Eds.), Thalassemia: Pathophysiology and Management, Part B (Alan R. Liss, New York, 1988), p. 81.
[3] D.K. Johnson, T.B. Murphy, N.J. Rose, L. Goodwind and W.H. Pickart, *Inorg. Chim. Acta* **67**, 159 (1982).
[4] L. Pickart, W.H. Goodwin, T.B. Murphy and D.K. Johnson, *Biochem. Pharmacol.* **32**, 3868 (1983).
[5] A.I. Vogel, A Text Book of Quantitative Inorganic Analysis (Longman, Suffolk, 1961).
[6] J.A. Well and J.K. Kinnai, *J. Phys. Chem.* **71**, 3341 (1967).
[7] M.A. El-Sayed, A.A. Yahia and A.M. Galap, *Heteroatom. Chem.* **10**, 1 (1999).
[8] G.M. Abu El-Reash, K.M. Ibrahim and M.M. Bekheit, *Transition Met. Chem.* **15**, 148 (1990).
[9] W.J. Geary, *Coord. Chem. Rev.* **7**, 81 (1971).
[10] B. Singh and P. Srivastava, *Transition Met. Chem.* **12**, 475 (1987).
[11] M.M. Mostafa, M.A. Khattab and K.M. Ibrahim, *Synth. React. Inorg. Met.-Org. Chem.* **14**, 39 (1984).
[12] M.A. Khattab, *Pakistan J. Sci. Ind. Res.* **23**, 114 (1980).
[13] K. Nakamoto, Infrared and Raman Spectra of Inorganic and Coordination Compounds (Wiley Interscience, New York, 1978), 3rd Edn.
[14] R.M. El-Shazely, M.S. Soliman, A.M. Shallaby and M.M. Mostafa, *Synth. React. Inorg. Met.-Org. Chem.* **23**, 301 (1990).
[15] R.G. Pearson, *J. Chem. Educ.* **45**, 581, 643 (1968).
[16] K.K. Narang, R.A. Lai, R.K. Thapa and V.K. Gautam, *Transition Met. Chem.* **13**, 212 (1988).
[17] R.C. Aggarwal, N.K. Singh and R.P. Singh, *Synth. React. Met.-Org. Chem.* **14**, 637 (1984).
[18] E. Sinn and C.M. Harris, *Coord. Chem. Rev.* **4**, 391 (1969).
[19] A.K. El-Sawaf, D.X. West, F.A. El-Saied and R.M. El-Bahnasawy, *Synth. React. Inorg. Met.-Org. Chem.* **27**, 1127 (1997).
[20] S.M. Abu-El-Wafa, A. Salibk, G. El-many and T.M. Ismial, *Synth. React. Inorg. Met.-Org. Chem.* **20**, 1343 (1990).
[21] A.B.P. Lever, Inorganic Electronic Spectroscopy (Elsevier, New York, 1968), p. 335.
[22] G.C. Chiumia, D.J. Phillips and A.D. Rae, *Inorg. Chim. Acta* **238**, 197 (1995).
[23] A.B.P. Lever, *Inorg. Chem.* **4**, 1042 (1965).
[24] E. Gao, S. Bi, H. Sun and S. Liu, *Synth. React. Inorg. Met.-Org. Chem.* **27**, 1115 (1997).
[25] E.W. Ainscough, A.M. Brodie, A.J. Dobbs, J.D. Ranford and J.M. Water, *Inorg. Chim. Acta* **267**, 27 (1998).
[26] V. Ravindar, S.J. Swamy, S.S. Srihari and P. Longaiah, *Polyhedron* **4**, 1511 (1985).
[27] E. Gao, S. Bi, H. Sun and S. Liv, *Synth. React. Inorg. Met.-Org. Chem.* **27**, 115 (1997).
[28] T.I. Kasher, A.S. El-Tabl and R. El-Bahnasawy, *Polish J. Chem.* **72**, 2037 (1998).
[29] A.S. El-Tabl, MSc Thesis (Menoufia University, Egypt, 1987).
[30] B.N. Figgis and J. Lewis, *Prog. Inorg. Chem.* **6**, 37 (1967).
[31] A.S. El-Tabl, PhD Thesis (Menoufia University, Egypt, 1993).
[32] Y. Kumar, *Synth. React. Inorg. Met.-Org. Chem.* **20**, 13 (1990).
[33] A.Z. El-Sonbati, *Transition Met. Chem.* **16**, 45 (1991).
[34] S. Jayasree and K.K. Aravindakshan, *J. Indian Chem. Soc.* **71**, 97 (1994).
[35] J.C. Eisenstein, *J. Chem. Phys.* **28**, 323 (1958).
[36] B.J. Hathaway and T.E. Billing, *Coord. Chem. Rev.* **5**, 143 (1970).
[37] M. Mahajan, K.N. Saxena and C.P. Saxena, *J. Inorg. Nucl. Chem.* **43**, 2148 (1981).
[38] A.S. El-Tabl, *Transition Met. Chem.* **21**, 1 (1996).
[39] I.M. Procter, B.J. Hathaway and P. Nicholls, *J. Chem. Soc. A* 1678 (1969).
[40] R.K. Ray, *Inorg. Chem. Acta* **174**, 237 (1990).
[41] R.K. Ray, *Inorg. Chim. Acta* **174**, 257 (1990).
[42] J.M. Assour, *J. Chem. Phys.* 4377 (1965).
[43] A.S. El-Tabl, T.I. Kashar, R. El-Bahnasawy and I.A. E1-Monsef, *Polish J. Chem.* **73**, 245 (1999).
[44] A.S. El-Tabl, *Transition Met. Chem.* **27**, 166 (2002).
[45] A.S. El-Tabl and T.I. Kashar, *Polish J. Chem.* **72**, 519 (1998).
[46] A.S. El-Tabl, *J. Chem. Res.* **529** (2002).
[47] A.S. El-Tabl, *Transition Met. Chem.* **23**, 63 (1998).
[48] D. Kivelson and R. Neiman, *J. Chem. Phys.* **40**, 365 (1964).
[49] D.W. Smith, *J. Chem. Soc. A* 3108 (1970).
[50] M. Shazly, A. Dissowky, T. Salem and M. Osman, *Inorg. Chem. Acta* **40**, 1 (1980).
[51] B.A. Goodman and J.B. Raynor, *Adv. Inorg. Chem. Radiochem.* **13**, 135 (1970).
[52] S. Chandra and K. Gupta, *Transition Met. Chem.* **27**, 196 (2002).

[53] W.W. Wendlandt, *J. Inorg. Nucl. Chem.* **25**, 833 (1963).
[54] M. Gaber and M.M. Ayad, *Therm. Chem. Acta* **176**, 21 (1991).
[55] A.S. El-Tabl and S.M. Imam, *Transition Met. Chem.* **22**, 259 (1997).
[56] A.S. El-Tabl and M.M. Abou-Sekkina, *Polish J. Chem.* **73**, 1937 (1999).
[57] K.Z. Ismail and A. El-Dissouky, *Polyhedron* **16**, 2909 (1997).